Theoretical estimates of the neutron production in the Columbia University shock tube, for a shock speed of 100 cm/μsec, predicted about 4×10^5 neutrons. Four 1B85 thyrode Geiger tubes, wrapped in 10-mil silver sheet and covered with a polyethylene moderator, were placed about the 50-cm point on the shock tube. For slightly slower shock speeds than shown in Table I no neutrons were observed. However, for the shock speeds indicated in Table I, neutrons have been detected, and by using a Los Alamos calibration[7] for this detector, we estimate a yield of about 5×10^5 neutrons. However, the close agreement between predictions and this measurement is thought to be more fortuitous than an indication of accuracy. A pilot B scintillator, shielded by 1 in. of lead, detected a burst of radiation which may be neutrons or nonthermal hard x rays. We do not know yet whether the neutrons are truly of thermonuclear origin.

The experimental data indicate that the shock-created plasma volume of $\sim10^4$ cm^3 has an internal energy density (nkT) of about 1.2 J/cm^3, a macroscopic kinetic energy ($\frac{1}{2}\rho V^2$) of about 2.8 J/cm^3, and that about 20% of the energy originally stored in the high-voltage capacitor bank was transferred into the plasma in the first half-cycle of the current pulse.

We acknowledge the many contributions by Dr. B. Miller in the design and early development of the shock tube, and thank Mr. M. Cea, Mr. J. Osarczuk, Mr. J. Ivers, and Mr. G. Beshara for its construction. We acknowledge many enlightening discussions with Dr. C. K. Chu, Dr. R. Taussig, and Dr. B. P. Leonard.

*Research supported by the U. S. Air Force Office of Scientific Research under Contract No. AF 49(638)-1634.

[1]R. A. Gross, Rev. Mod. Phys. 37, 724 (1965).

[2]C. K. Chu and R. A. Gross, in *Advances in Plasma Physics*, edited by A. Simon and W. B. Thompson (Wiley, New York, 1969), Vol. 2, p. 139.

[3]R. Kh. Kurtmullaev, Yu. E. Nesterikhin, V. I. Pil'skii, and R. Z. Sagdeev, in *Proceedings of the Second International Conference on Plasma Physics and Controlled Nuclear Fusion Research, Culham, England, 1965* (International Atomic Energy Agency, Vienna, Austria, 1966).

[4]L. S. Levine, I. M. Vitkovitsky, and A. C. Kolb, in Proceedings of the Seventh International Shock Tube Symposium, University of Toronto, Toronto, Canada, 1969 (to be published).

[5]R. A. Gross and B. Miller, in Methods in Experimental Physics: Plasma Physics, edited by H. R. Griem and R. H. Lovberg (to be published by Academic, New York, 1970), Vol. IX, Part A.

[6]S. Schneider, C. K. Chu, and B. P. Leonardi, private communication.

[7]R. J. Lanter and D. E. Bannerman, LASL Report No. LA 3498-MS, 1966 (unpublished).

BRAGG REFLECTION OF LIGHT FROM SINGLE-DOMAIN CHOLESTERIC LIQUID-CRYSTAL FILMS

D. W. Berreman and T. J. Scheffer
Bell Telephone Laboratories, Murray Hill, New Jersey 07974
(Received 6 July 1970)

Reflection measurements have been made for the first time on single-domain cholesteric liquid-crystal films. We observed spectral structure and polarization character with obliquely incident light never seen with the previously studied disordered films. We also obtained numerical solutions to Maxwell's equations for obliquely incident light in such materials by a new method. Our reflectivity measurements agree fairly well with computations based on Oseen's spiraling-dielectric-ellipsoid optical model for cholesteric systems.

Almost all previous optical studies of cholesteric liquid-crystal films were made on systems composed of cholesterol-derived molecules. The optical properties of these films were qualitatively explained by assuming a distribution in orientation of Bragg scattering domains embedded in a matrix of constant refractive index.[1] Adams and co-workers have shown that, among other difficulties, inhomogeneity in Bragg spacing makes it impractical to measure this angular distribution.[2] Because of this uncertainty in these materials no quantitative comparison can be given with the theories of Oseen,[3] De Vries,[4] and others,[5,6] who have derived optical equations for propagation and reflection in perfectly ordered samples.

We have avoided these experimental problems by studying the optical properties of a single domain of a cholesteric system in which the helicoidal axis is uniformly perpendicular to the

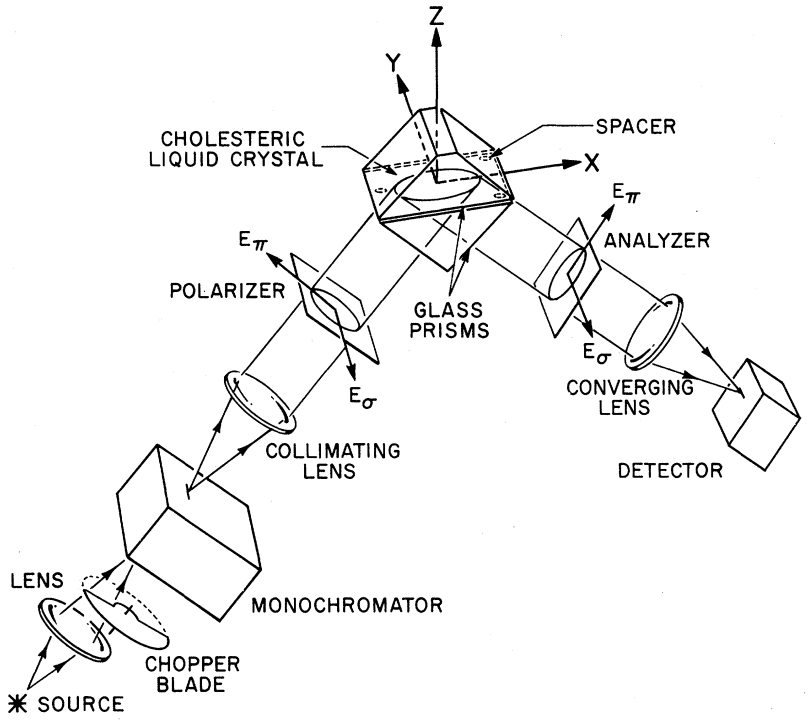

FIG. 1. Apparatus for measuring reflectance of oblique rays by a liquid-crystal film.

film surface over domains of 1 cm^2 or more. We have observed new features in the reflection bands of these cholesteric liquid-crystal films which could not be seen so clearly, if at all, in the previously studied disordered system.

Our cholesteric film consists of a binary mixture of non-mesomorphic, optically active 4, 4′-bis(2-methylbutoxy)azoxybenzene (2 MBAB) and nematic 4, 4′-bis(hexyloxy)azoxybenzene.[7] The pitch of the resulting cholesteric mesophase can be varied from infinity to 0.24 μm simply by increasing the mole fraction of 2 MBAB in the mixture from 0 to 85%, which is the upper limit for the existence of a pure cholesteric phase. The pitch shows only a small temperature dependence, decreasing only a few tenths of a percent for each centigrade degree temperature increase. The mosomorphic range depends upon the mole fraction of 2 MBAB, but all the ranges fall between 42 and 130°C.

Figure 1 shows the experimental arrangement we used to observe Bragg reflection. A parallel beam of plane-polarized monochromatic light is directed at 45° to the liquid-crystal film sandwiched between the faces of two $36\times25\times25$-mm^3 right-angle glass prisms. The part of the beam that is not transmitted through the film is specularly reflected through an analyzer into a photomultiplier detector. The reflected intensities are compared with 100% reflection values taken in a separate experiment using a single clean prism in the same geometry.

A temperature-controlled oven is placed around the prisms to keep the cholesteric film in its mesomorphic range. Spacers were made by evaporating chromium and electroplating chromium and gold at three spots on the lower prism face, and then polishing them to the desired thickness. The sample thickness was determined by measuring the wavelengths of a series of interference minima observed within an air bubble trapped in the film. The cholesteric pitch was calculated from the Grandjean plane spacings produced by placing some of the liquid crystal between a lens surface of known curvature and a flat glass plate.

To obtain a well-ordered film it is necessary to define the molecular orientation at the surfaces of the film. This is accomplished by cleaning and then rubbing the faces of both prisms on lens tissue in the x direction (see Fig. 1). The sample is introduced in the isotropic phase between the heated prisms and the system is allowed to cool into the cholesteric range. Final alignment is obtained by working the upper prism back and forth several times in the x direction.

Our sample contained several parallel Grandjean discontinuities about 1 cm apart because it

was slightly wedge shaped. In order to take reflectivity measurements over a region of uniform pitch, a mask was positioned so that only light from a $2\times\frac{1}{2}$-mm rectangular area, halfway between the discontinuities of the film and parallel to them, was allowed to strike the detector.

Recently Taupin[6] published a method for solving Maxwell's equations for light propagating obliquely through a liquid crystal described by Oseen's dielectric model. He obtained approximate solutions for reflectance by semi-infinite crystals by solving a truncated infinite set of simultaneous equations. We developed a very different method analogous to numerical integration through the sample, as in De Vries's paper,[4] but with a 4×4-matrix multiplication at each step of the integration. Our method is easy to use with more general optical models and with films.

Suppose the dielectric properties of a medium can be represented locally by a symmetric dielectric tensor ϵ, and that the medium is nonmagnetic, so that the permeability is unity in Gaussian units. Consider plane-wave solutions to Maxwell's equations, such that there is no dependence on the y coordinate and the x coordinate and time dependence are represented by a factor $\exp[i(kx-\omega t)]$. It is not difficult to verify that, under these circumstances, Maxwell's equations can be reduced to the matrix form:

$$\frac{\partial}{\partial z}\begin{pmatrix} E_x \\ iH_y \\ E_y \\ -iH_x \end{pmatrix} = \frac{\omega}{c}\begin{pmatrix} -i\left(\frac{kc}{\omega}\right)\frac{\epsilon_{xz}}{\epsilon_{zz}} & 1-\frac{1}{\epsilon_{zz}}\left(\frac{kc}{\omega}\right)^2 & -i\left(\frac{kc}{\omega}\right)\frac{\epsilon_{yz}}{\epsilon_{zz}} & 0 \\ -\epsilon_{xx}+\frac{\epsilon_{xz}^2}{\epsilon_{zz}} & -i\left(\frac{kc}{\omega}\right)\frac{\epsilon_{xz}}{\epsilon_{zz}} & \frac{\epsilon_{xz}\epsilon_{yz}}{\epsilon_{zz}}-\epsilon_{xy} & 0 \\ 0 & 0 & 0 & 1 \\ \frac{\epsilon_{xz}\epsilon_{yz}}{\epsilon_{zz}}-\epsilon_{xy} & -i\left(\frac{kc}{\omega}\right)\frac{\epsilon_{yz}}{\epsilon_{zz}} & \frac{\epsilon_{yz}^2}{\epsilon_{zz}}-\epsilon_{yy}+\left(\frac{kc}{\omega}\right)^2 & 0 \end{pmatrix}\begin{pmatrix} E_x \\ iH_y \\ E_y \\ -iH_x \end{pmatrix}$$

or

$$\partial\psi/\partial z = (\omega/c)\overleftrightarrow{\mathfrak{D}}\psi. \tag{1}$$

An optical model, of which those of Oseen[3] and others[4-6] are a special case, is described by the z-coordinate-dependent dielectric tensor in which

$$\begin{aligned} \epsilon_{xx} &= \bar{\epsilon}+\tfrac{1}{2}\delta\epsilon\cos\alpha z, \\ \epsilon_{yy} &= \bar{\epsilon}-\tfrac{1}{2}\delta\epsilon\cos\alpha z, \\ \epsilon_{xy} &= \epsilon_{yx} = \tfrac{1}{2}\delta\epsilon\sin\alpha z, \\ \epsilon_{zz} &= \epsilon_3, \end{aligned} \tag{2}$$

and all other tensor components are zero. This dielectric tensor can be represented by an ellipsoid in which the ϵ_3 principal axis is always parallel to the z coordinate, and the two other principal axes, $\bar{\epsilon}+\frac{1}{2}\delta\epsilon$ and $\bar{\epsilon}-\frac{1}{2}\delta\epsilon$, spiral around the z-coordiante axis with pitch $4\pi/\alpha$ (see Fig. 2). This optical model has no optical activity in the usual sense[8] since it is described locally by a real symmetric ϵ tensor and a unit μ tensor. Nevertheless, plane-polarized light transmitted through the film may come out approximately plane polarized in a new direction. This same sort of rotary effect was demonstrated long ago by E. Reusch[9] with a spiraling pile of anisotropic, but optically inactive, mica sheets.

Oseen[3] and others[4,5] found only the equivalent of the eigenvectors and eigenvalues of our matrix equations for the special case when $k=0$. Hence ϵ_3 does not appear in their solutions. Conners[5] is the only researcher who obtained solutions for finite films in that case. Taupin[6] found solutions for light obliquely incident on semi-infinite samples.

For the special case $k=0$, when light is norm-

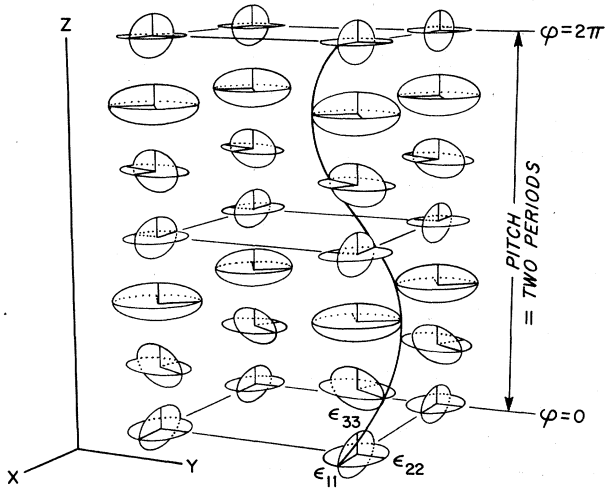

FIG. 2. Spiraling dielectric ellipsoids in Oseen's optical model of a cholesteric liquid crystal.

ally incident on the film, there is only one forbidden band for transmission of light, corresponding to a single order of Bragg reflection. This result was first obtained by Oseen[3] and later by De Vries.[4] However, when light is incident obliquely on a perfectly ordered film, second- and higher-order reflection bands make their appearance.[6] The higher-order bands increase in strength as k, or the angle of incidence, increases. All bands are triplets when $k \neq 0$.

Our numerical method of solution can only be briefly outlined here. We note that for very small intervals δz, we could write the approximate expression

$$\psi(z+\delta z) \equiv \overleftrightarrow{P}(z, \delta z)\psi(z) \approx [\overleftrightarrow{1} + (\omega/c)\delta z \overleftrightarrow{\mathfrak{D}}(z)]\psi(z), \quad (3)$$

where $\overleftrightarrow{P}$ is a 4×4 "propagation" matrix, and where $\overleftrightarrow{1}$ is the unit 4×4 matrix. Repeated matrix multiplication by very small steps δz across the film thickness would give a matrix $\overleftrightarrow{T}(\Delta z)$ for the total film thickness Δz, which relates the electromagnetic field vector ψ at one side of the liquid-crystal film to that at the other.

Knowing the wave function of the incident light ψ_i, and the matrix $\overleftrightarrow{T}$ for the liquid-crystal film and the properties of the confining media (glass prisms in this case), we can solve for the wave function of the reflected and transmitted light (ψ_r and ψ_t) using four simultaneous linear equations. The eight variables in ψ_r and ψ_t are first reduced to four by using the known relations between E and H in the confining media outside the film. Eigenvalues and eigenvectors of $\overleftrightarrow{T}$ when Δz is one pitch length are equivalent to Taupin's propagated wave solutions.

Actually, the approximation for $\overleftrightarrow{P}$ in Eq. (3) does not converge to $\overleftrightarrow{T}$ in general. One way to get a convergent multiplicative series is to modify the first-order expression for $\overleftrightarrow{P}$ with second-order terms in δz such that it has the necessary symmetry property $\overleftrightarrow{P}(z, \delta z) = \overleftrightarrow{P}^{-1}(z, -\delta z)$. Cyclic and other symmetry properties of $\overleftrightarrow{\mathfrak{D}}(z)$ also allow us to abbreviate the repeated matrix-multiplication process to around 100 matrix multiplications for any reasonable film thickness. It is also possible to find an exact mathematical expression for the matrix $\overleftrightarrow{P}$ over any finite interval Δz when the z-dependent part of $\overleftrightarrow{\mathfrak{D}}$ is missing (i.e., when $\delta\epsilon = 0$) by taking a limit as the number of multiplicative interactions with Eq. (3) goes to infinity over a finite interval Δz. We used this exact matrix, $\overleftrightarrow{P}_0(\Delta z)$, in finding matching solutions in the glass on either side of the liquid crystal. We also used it to obtain a rapidly converging expression in place of the simple first-order approximation shown in Eq. (3), within the liquid crystal, by treating the effect of $\delta\epsilon$ as a correction, but not a small perturbation, on the propagation.

The technique outlined here was used to generate reflectance spectra for liquid-crystal films having the known thickness and pitch of our samples. By adjusting $\bar{\epsilon}$, $\delta\epsilon$, and ϵ_3 we were able to fit frequencies of variations in reflectance quite closely (see Fig. 3). The method can easily be used for models with dielectric tensors that vary in a more complicated way. Our experimental data did not show additional Bragg reflection bands or other spectral features that we predicted if the principal axis ϵ_3 was not parallel to the z axis. We found that $\epsilon_3 \approx \bar{\epsilon} - \frac{1}{2}\delta\epsilon$; that is, that the dielectric tensor ellipsoid is (at least approximately) a prolate spheroid, as assumed by Taupin.[6] Our computations show that the second-order Bragg reflection band for an oblate

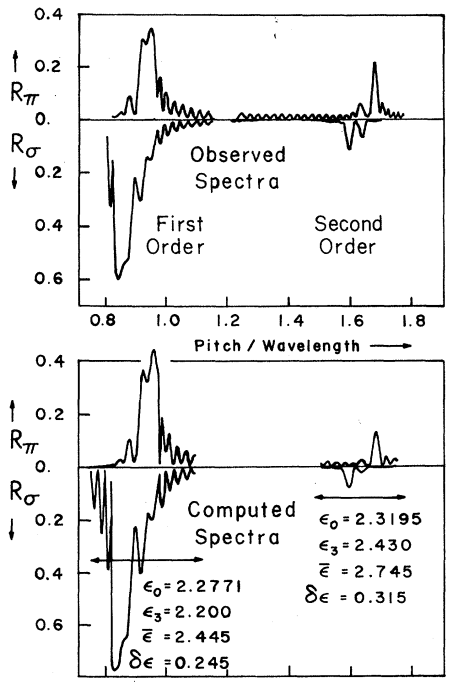

FIG. 3. First- and second-order reflectance spectra of a cholesteric liquid-crystal film 15 pitch lengths or 11.47 μm thick, confined between two glass prisms of optical dielectric constant ϵ_0. Light beam is incident at 45 deg. Polarizer and analyzer were parallel to the plane of reflection for R_π and normal to it for R_σ measurements. Mole fraction of 2 MBAB is 0.45 and temperature is 88°C. Small oscillations are interference fringes from the two film-prism interfaces.

spheroid would be much less symmetric about the central component of the band (which is common to both π- and σ-polarized radiation) than that computed for a prolate spheroid.

We believe that the discrepancy between computed and measured intensities shown in Fig. 3 is significant. The first-order Bragg reflection band is somewhat weaker, and the second order is stronger, than predicted. Altering the initial and final aximuth of the dielectric ellipsoid or its principal values only made the fit worse. Assuming an error in pitch measurement did not help either. Thin regions near the surfaces with anomalous dielectric properties might account for the discrepancy.

F. Unterwald contributed valuable technical assistance.

[1]J. L. Fergason, Mol. Cryst. 1, 293 (1966).
[2]J. E. Adams, W. Haas, and J. Wysocki, J. Chem. Phys. 50, 2458 (1959).
[3]C. W. Oseen, Trans. Faraday Soc. 29, 833 (1933).
[4]H. De Vries, Acta Cryst. 4, 219 (1951).
[5]G. H. Conners, J. Opt. Soc. Amer. 58, 875 (1968).
[6]D. Taupin, J. Phys. (Paris) 30, C4-32 (1969).
[7]E. Sackmann, S. Meiboom, and L. C. Synder, J. Amer. Chem. Soc. 89, 5981 (1967).
[8]P. Drude, *Theory of Optics* (Longmans, Green, New York, 1902), Chaps. 6, 7.
[9]F. A. Jenkins and H. E. White, *Fundamentals of Optics* (McGraw-Hill, New York, 1957), 3rd ed., p. 584.

PHOTOEMISSION STUDIES OF FERROMAGNETIC AND PARAMAGNETIC NICKEL*

D. T. Pierce and W. E. Spicer
Stanford Electronics Laboratories, Stanford University, Stanford, California 94302
(Received 16 March 1970)

High-resolution photoemission spectra obtained from ferromagnetic nickel (295°K, $0.47T_C$) and paramagnetic nickel (678°K, $1.07T_C$) give no evidence of a change in the position of the d-electron peak near the high-energy cutoff of the photoelectron distribution within the experimental uncertainty of ±0.05 eV. On the other hand, a calculation of the spectra based on a band structure with an exchange splitting of 0.37 eV for ferromagnetic Ni and zero splitting for paramagnetic Ni predicted peak position changes of 0.1 to 0.2 eV.

We report the first high-resolution photoemission measurements above and below the Curie temperature of a ferromagnetic metal in the $3d$ transition series. An attempt was made to detect any differences between the electronic structure of ferromagnetic and paramagnetic Ni by obtaining photoemission spectra of 295°K where the magnetization of nickel is 95% of its maximum value and at 678°K where the magnetization is zero. Any effect of spin ordering on photoemission spectra would be most apparent for such a large difference in magnetization rather than for a small difference in magnetization at temperatures just above and just below the Curie temperature ($T_C = 631$°K). The strongest structure in the photoelectron energy-distribution curve (EDC) is a peak near the high-energy cutoff due to electrons originating in d bands near the Fermi energy E_F. The position of this peak was found to be the same at both 295 and 678°K within the experimental uncertainty of ±0.05 eV.

In contrast to the experimental results, our calculations of EDC's for ferromagnetic and paramagnetic Ni predicted 0.1- to 0.2-eV differences in the position of the main peak. The difference in energy between electron states of opposite spin is manifested in the exchange splitting of the spin-up and spin-down bands which has been estimated for Ni by Wohlfarth[1] as 0.35 ± 0.05 eV and by Phillips[2] as 0.5 ± 0.1 eV. We calculated photoemission energy-distribution curves using the interpolated energy bands of Hodges, Ehrenreich, and Lang[3] with an exchange splitting of 0.37 eV at E_F. We assumed the paramagnetic state could be represented by unsplit bands as is conventional in paramagnetic band calculations[4,5] and models of magnetism where the exchange splitting is proportional to the magnetization.[6,7]

The experimental results reported here were obtained from a sample which was prepared by electron-gun evaporating a Ni film ~1500-Å thick onto a single-crystal Ni substrate. The pressure rose from a base pressure of 1×10^{-11} Torr to 1×10^{-9} Torr during the initial stages of evaporation (2 min) but remained less than 5×10^{-10} Torr during the rest of the evaporation (17 min). Lack of surface contamination was established by the absence of a low-energy peak of scattered